

Numerical study of axisymmetrical transsonic impact based on the SST turbulence model

Erkin Madaliev^{1*}, *Murodil Madaliev*^{1,2}, *Bakhodir Mirzaev*¹, *Farangiz Tillaboyeva*¹, *Akmaljon Mamatov*¹, *Sherzodjon Ro'zaliyev*³, and *Zilolaxon Mamatova*³

¹Fergana Polytechnic Institute, 86, Fergana Street, 150107, Fergana, Uzbekistan

²Institute of Mechanics and Seismic Resistance of Structures of the Academy of Sciences of the Republic of Uzbekistan, Tashkent, Uzbekistan

³Fergana State University, 19, Murabbiylar Street, Fergana, 111000, Uzbekistan

Abstract. This study presents a comprehensive numerical simulation of the aerodynamic behavior of an axisymmetric model featuring a spherical convex radome at transonic Mach numbers, employing the Comsol Multiphysics software package for advanced computational analysis. The primary focus is on the shock wave dynamics that develop at the upper section of the spherical convex fairing, a critical aspect for understanding the aerodynamic performance and stability of aerospace vehicles. By simulating various conditions, the study seeks to capture the intricate interactions between the incoming airflow and the radome structure, which are crucial for optimizing design parameters. The numerical results obtained are rigorously compared with experimental data from the research conducted by Bachalo and Johnson, illustrating a close alignment that reinforces the accuracy and reliability of the numerical calculations. These simulations utilize the Shear Stress Transport (SST) turbulence model, which is adept at handling complex flow features, further validating the significance of these findings for future aerospace applications.

1 Introduction

Turbulence is one of the most complex phenomena of classical physics, which still remains a mystery. The complex and chaotic nature of turbulent flows makes the current physical understanding of this phenomenon incomplete. Computational fluid dynamics (CFD)-based models are used to predict turbulent flows. However, due to a lack of fundamental knowledge of physics, one has to resort to dimensional analysis and other methods to determine the coefficients that are used in these models (called "closure coefficients"). The choice of numerical values of these coefficients is based on a combination of heuristic and empirical approaches. Although model developers usually try to validate their choices based on experimental data, the universality of such models for all possible turbulent flows cannot be guaranteed [1–3].

* Corresponding author: Madaliev.me2019@mail.ru

In aerodynamics and fluid dynamics, numerical modeling plays a key role in the study and understanding of complex flow processes. It is especially important to understand the behavior of flows near bodies with changing geometry, such as spherical convex radomes. In this study, we focus on an axisymmetric model with a spherical hump, examining its behavior at transonic Mach numbers. The use of numerical methods, such as the Comsol Multiphysics software package, allows detailed studies to be carried out, providing a unique opportunity to analyze flow characteristics under various conditions.

An outstanding example of shock wave research is the work carried out by Bachalo and Johnson in the early 1980s [4]. In their experiment, measurements were performed at high subsonic Mach numbers over an axisymmetric protrusion on a cylindrical body. This protrusion was intended to create an unsteady separation caused by the shock wave. Near the top of the hump, the flow becomes supersonic, forming a weak shock wave, which creates an unfavorable pressure gradient on the oncoming boundary layer. This causes the boundary layer to detach, forming a transient separation bubble downstream of the hump, which then undergoes unstable reattachment. Figure 1 illustrates the Bachalo-Johnson experimental apparatus. The PIV technique was used to obtain these data; axis and contour labels were removed from the images to prevent disclosure of relevant information prior to testing [5–10].

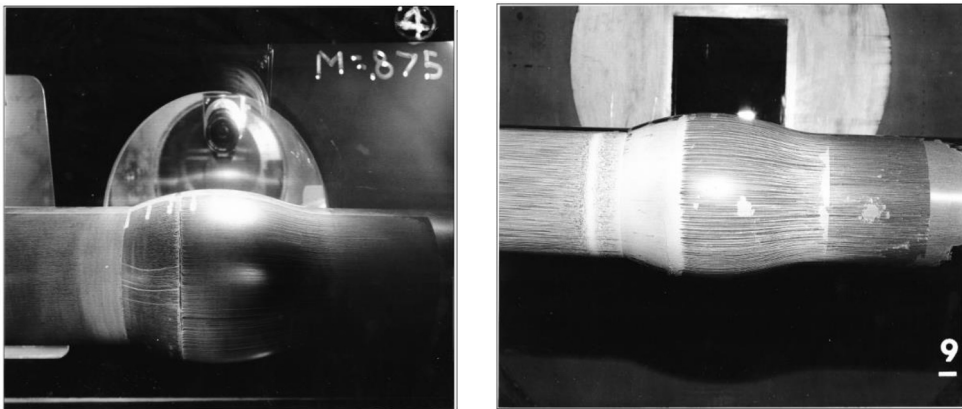


Fig. 1. Bachalo-Johnson experimental device.

The purpose of this study is to present the results of numerical simulation of transonic flow past a spherical convex radome using the Comsol Multiphysics software package. The main attention is paid to the analysis of the flow characteristics of the upper part of the bulge in order to gain a deeper understanding of its properties, including shock waves formed during the flow process. To confirm the accuracy and reliability of our numerical calculations, including the use of the SST turbulence model, a detailed study covering various flow regimes and flow parameters is carried out. The results obtained are presented in the form of graphical data, allowing a more complete assessment of the flow dynamics in the system under consideration. This analysis also includes an assessment of the influence of various parameters, such as flow speed and geometric characteristics of the streamlined body. The results obtained can have significant implications for the development of more efficient and optimized aerodynamic designs in various fields of engineering and technology. In addition, this study can contribute to the further development of numerical modeling methods in aerodynamics by exploring and optimizing various numerical schemes and algorithms used to solve such problems [11, 12].

2 Physical and mathematical formulation of the problem

The geometry of the axisymmetric protrusion and the computational mesh is shown in Figure 2. The free-stream Mach number is $M = 0.875$ and the Reynolds number calculated from the chord length of the protrusion is $Re_c = 2.763$ million. The experiment of Bachalo and Johnson [4] shows that flow separation occurs after the shock wave on the ledge. Oil flow visualization shows that flow separation and reattachment occur at $x/c = 0.7$ and 1.1 , respectively.

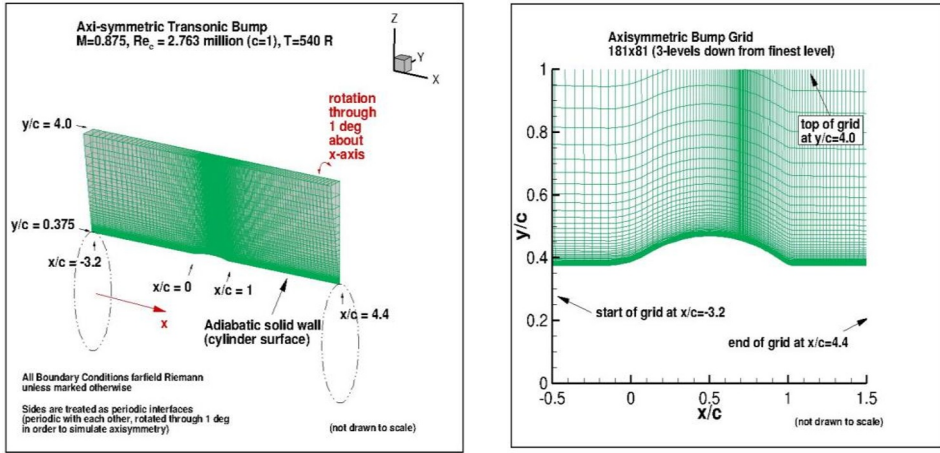


Fig. 2. The geometry of the axisymmetric protrusion and the computational mesh is shown.

3 Mathematical model

To study the flow around an axisymmetric protrusion, the Reynolds-averaged Navier-Stokes equations were applied. These equations represent the basis for the mathematical description of the movement of an incompressible fluid and are a system of differential equations that describe the change in speed and pressure inside a liquid medium depending on time and coordinates. Reynolds averaging allows one to take into account the effect of turbulence on the flow, while simplifying the solution of equations and reducing the computational complexity of the problem [13–18].

The Navier-Stokes equations in averaged form take into account turbulent flows and represent the following system of equations:

Mass conservation equation (continuity equation), which describes the law of conservation of mass within the computational domain:

$$\frac{\partial \bar{u}_i}{\partial x_i} = 0 \tag{1}$$

The momentum conservation equation, which describes the change in fluid velocity under the influence of external and internal forces:

$$\frac{\partial \bar{u}_i}{\partial t} + \bar{u}_j \frac{\partial \bar{u}_i}{\partial x_j} = -\frac{1}{\rho} \frac{\partial \bar{p}}{\partial x_i} + \nu \frac{\partial^2 \bar{u}_i}{\partial x_j \partial x_j} + \frac{\partial \tau_{ij}}{\partial x_j} \tag{2}$$

where

\bar{u}_i - components of the mean velocity field, \bar{p} - average pressure, ν - kinematic viscosity, τ_{ij} - stress tensor components, ρ - density. In transonic flow, the gas density changes. To find the density, the energy transfer equation is used. In transonic flow, the gas density changes. To find the density, the energy transfer equation is used.

For a compressible fluid, the energy transfer equation takes into account changes in the internal energy of the fluid in response to changes in pressure and temperature. The formulation of the energy equation for a compressible fluid is as follows:

$$C_p \rho \left(\frac{\partial T}{\partial t} + \bar{u}_j \frac{\partial T}{\partial x_j} \right) = \frac{\partial}{\partial x_j} \left(\lambda \frac{\partial T}{\partial x_j} \right) + \frac{\mu}{Pr} \left(\frac{\partial}{\partial x_j} \left(\frac{\partial T}{\partial x_j} \right) \right) - \frac{P}{\rho} \left(\frac{\partial \bar{u}_j}{\partial x_j} \right) + Q. \quad (3)$$

ρ - fluid density,

C_p - specific heat capacity at constant pressure,

T - temperature,

t - time,

u - velocity vector,

λ - thermal conductivity coefficient,

μ is the dynamic viscosity of the liquid,

Pr - Prandtl number (the ratio of the viscosity coefficient to the thermal conductivity coefficient),

P - pressure,

Q is the heat source.

This equation describes the change in temperature in a compressible fluid in time and space, and also includes additional terms to account for compressibility effects such as pressure work and thermal conductivity.

The use of the Reynolds-averaged Navier-Stokes equations makes it possible to take into account turbulent effects and their influence on the flow around an axisymmetric protrusion. The solution of these equations is carried out using numerical methods such as the finite element method. For this purpose, specialized software packages are often used, for example, Comsol Multiphysics. This approach provides detailed flow characteristics and is an effective tool for analyzing and modeling complex turbulent flows [19, 20].

4 Turbulence models

The SST (Shear Stress Transport) model [21–26] is one of the most widely used turbulence models in the numerical simulation of aerodynamic flows. It is a combination of two turbulence models: the k- ω model (kinetic energy viscosity component) in the near boundary layer and the k- ϵ model (kinetic energy dissipation viscosity component) in the distant boundary layer. This combination allows various aspects of turbulent flow to be more effectively taken into account and improves the accuracy of numerical simulations of aerodynamic phenomena.

$$\begin{cases} (\mathbf{U} \cdot \nabla) k = \nabla[(v + \sigma_k v_t) \nabla k] + P - \beta^* \omega k, \\ (\mathbf{U} \cdot \nabla) \omega = \nabla[(v + \sigma_\omega v_t) \nabla \omega] + \frac{\gamma}{v_t} P - \beta \omega^2 + 2(1 - F_1) \frac{\sigma_{\omega^2}}{\omega} \nabla \omega \nabla k. \end{cases} \quad (4)$$

Here k is the specific turbulent kinetic energy ($\text{m}^2 \text{s}^{-2}$), ω is the specific rate of turbulent dissipation (s^{-1}). Other values are presented in [21–26].

The Shear Stress Transport (SST) model is a powerful tool for numerical simulation of aerodynamic flows and has several advantages: **Versatility:** The SST model provides accurate prediction of turbulent effects in a wide range of flow regimes, including both laminar and turbulent flows. **Efficiency:** This model is particularly useful in simulating flow around airfoils and other complex geometries where different flow regimes are present. **Accuracy:** The SST model takes into account both the influence of viscosity in the near layer of the boundary and the effect of energy dissipation in the distant layer of the boundary, which allows a more accurate description of turbulent structures in the flow. **Popularity:** Due to its efficiency and accuracy, the SST model is one of the preferred choices for engineers and researchers involved in numerical simulation of aerodynamic flows.

Overall, the SST model provides an important tool for aerodynamic research and engineering calculations, providing high accuracy and reliability in a variety of conditions.

5 Solution method

To analyze turbulent flows in our study, we used the SST turbulence model available in the Comsol Multiphysics software package. Comsol Multiphysics provides a variety of solvers specifically designed for modeling a variety of physical phenomena, including aerodynamics and turbulent flows. These tools allow you to perform numerical simulations with high accuracy and efficiency, and provide the flexibility to adapt to different types of problems and geometries [27–33].

6 Results and its discussion

Figure 3 shows flow velocity contours and a streamline, which clearly demonstrate the flow velocity distribution. These contours allow us to visualize the main characteristics of the flow and identify areas of acceleration and deceleration around the protrusion [34–38].

Velocity contours help researchers and engineers better understand flow dynamics and their impact on the aerodynamic properties of a protrusion. Based on these data, it is possible to draw conclusions about the flow structure, areas of vortex formation, as well as determine potential flow areas and possible points of aerodynamic resistance.

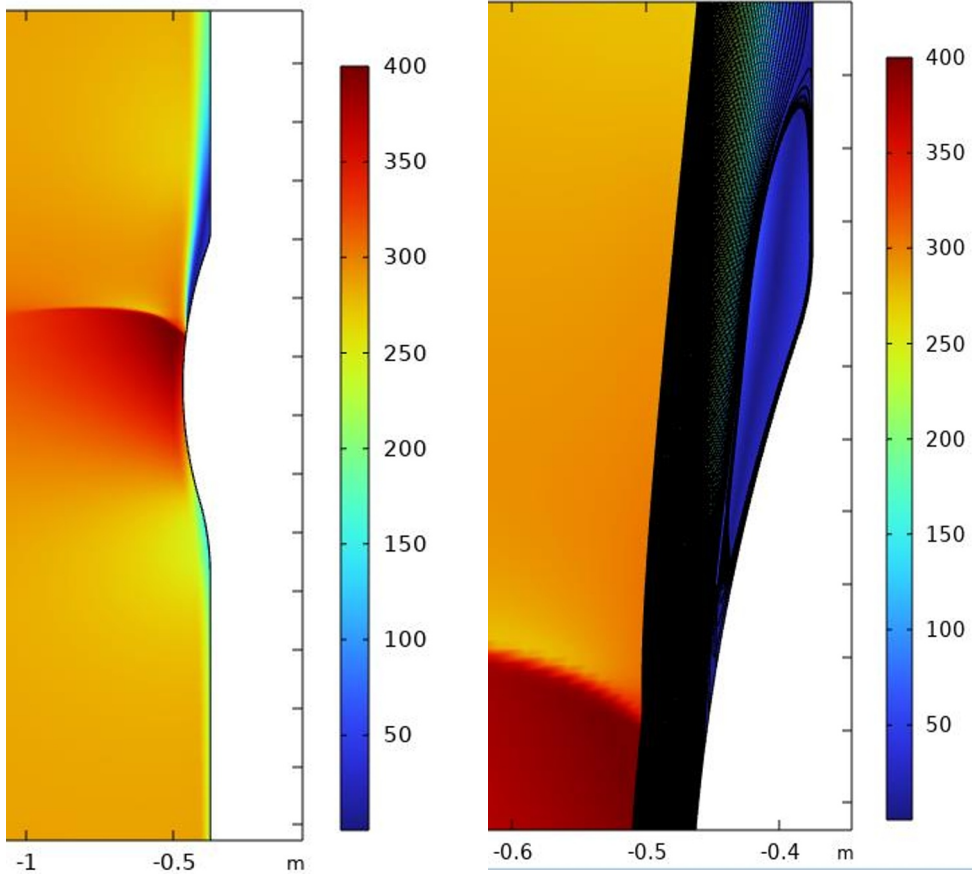


Fig. 3. Flow velocity contours and streamline around the protrusion.

In Figure 4 shows Mach number isolines, which clearly demonstrate the velocity distribution. These lines help visualize areas of different flow speeds and highlight areas where speeds reach transonic or supersonic values. Mach number contours are an important tool for analyzing the aerodynamic characteristics of an airfoil and determining the transition points of flow from one regime to another. They help researchers better understand the flow dynamics around a profile and identify areas where shock waves or other turbulent phenomena may occur.

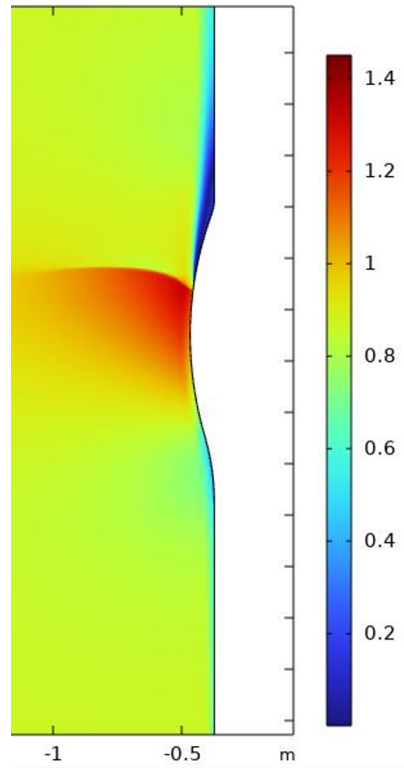


Fig. 4. Mach number isolines.

Figure 5 shows temperature distribution contours, which clearly illustrate how the temperature is distributed in the flow. These contour lines help visualize areas of high or low temperature and reveal thermal characteristics. Understanding temperature distribution helps researchers and engineers optimize designs for increased efficiency and improved thermal performance. Such visualizations can also be used to identify potential problem areas that require additional analysis and improvement [39–40].

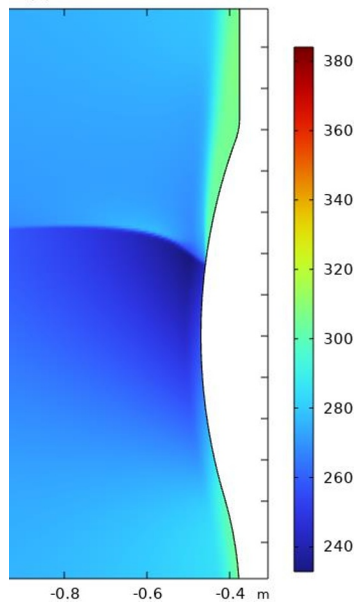


Fig. 5. Isolines of temperature distribution.

Figure 6 shows isolines of changes in air density, which clearly illustrate the density distribution. These contour lines help visualize areas where air density changes, which may be caused by temperature or speed changes in the flow.

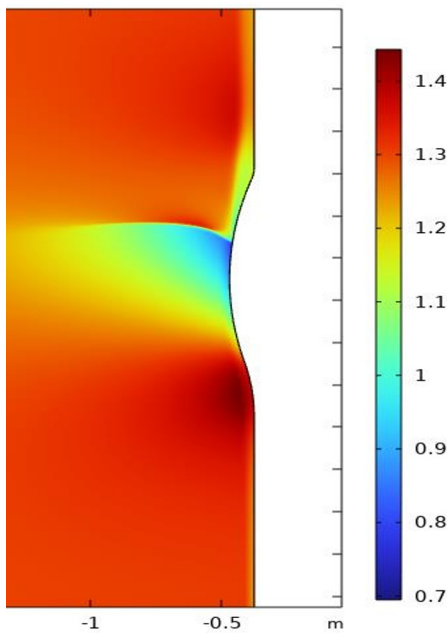


Fig. 6. Isolines of changes in air density.

In Figure 7 shows a comparison of the pressure coefficient on the profile surface obtained as a result of numerical modeling with experimental data. The pressure coefficient is an important parameter that characterizes the distribution of pressure along the airfoil

surface and affects its aerodynamic properties, such as lift and drag. The graph shows pressure coefficient curves that show the change in this parameter along the profile chord. The results of numerical simulations are indicated by solid lines, and the experimental data are indicated by diamonds.

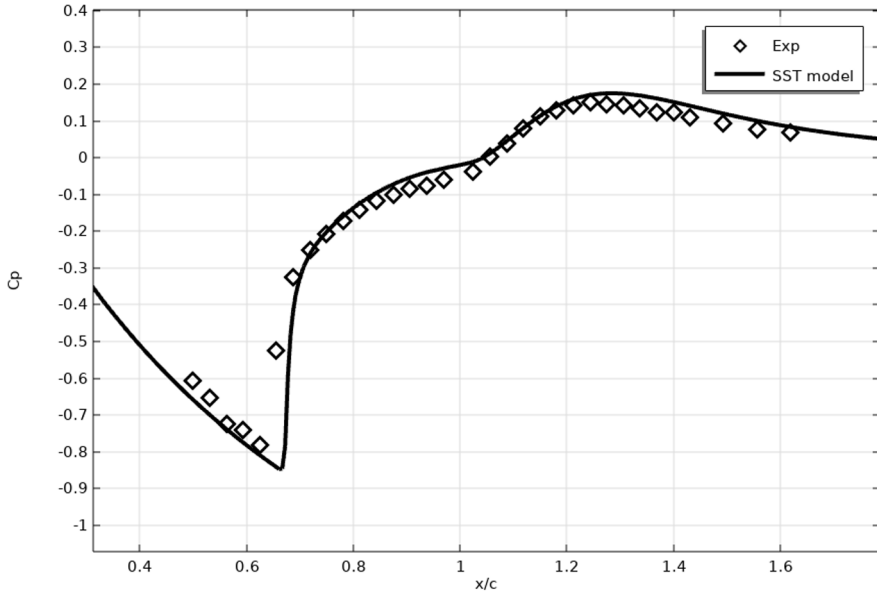


Fig. 7. Redemption surface pressure coefficient.

From Figure 7 it is obvious that the main discrepancy between the numerical and experimental data is observed precisely in the region of shock wave formation. This region plays a key role in aerodynamic behavior and therefore requires additional analysis to improve the accuracy of the numerical simulations.

7 Conclusion

The study demonstrated that turbulence and aerodynamic flow characteristics are complex phenomena that require careful analysis and modeling. Mach number contours and temperature distributions are important tools for visualizing and understanding these phenomena. In addition, it was found that the main discrepancy between the numerical and experimental data is observed in the region of shock wave formation. This highlights the need for further research and improvement of numerical modeling accuracy in this area. Thus, for a deeper understanding and successful prediction of aerodynamic processes, it is necessary to conduct additional research, taking into account the characteristics of turbulence and the influence of shock waves.

The authors conclude with this brief introduction and consider it a pleasant duty to express sincere gratitude to their teacher, professor of the Fluid mechanics laboratory Zafar Mamatkulovich Malikov, who inspired them with enthusiasm and interest in the study of turbulence.

References

1. E. Stanewsky et al. (eds.), EUROSHOCK - drag reduction by passive control design, Notes on Numerical Fluid Mechanics **56** (1997)

2. E. Stanewsky et al. (eds.), Drag reduction by shock and boundary layer control. Notes on Numerical Fluid Mechanics and Multi-Disciplinary Design **80** (2002)
3. M. Patzold et al., Numerical optimization of finite shock control bumps. AIAA 44th Aerospace Sciences Meeting and Exhibit, pp. 9–12 Reno (2006)
4. W. Bachalo, D. A. Johnson, AIAA Journal **24(3)**, 437-443 (1986)
5. D. Johnson, *Predictions of transonic separated flow with an eddy-viscosity/Reynolds-shear-stress closure model*, in Proceedings of the 18th Fluid Dynamics and Plasmadynamics and Lasers Conference, p. 1683 (1985)
6. D. A. Johnson, AIAA Journal **25(2)**, 252-259 (1987)
7. M. Madaliev et al., E3S Web of Conferences **538**, 01012 (2024)
8. M. Madaliev et al., E3S Web of Conferences **538**, 01019 (2024)
9. M. Madaliev et al., E3S Web of Conferences **538**, 01013 (2024)
10. M. Madaliev et al., E3S Web of Conferences **538**, 01018 (2024)
11. X. Han et al., *Wall-distance free wray-agarwal turbulence model with elliptic blending*, in Proceedings of the 2018 Fluid Dynamics Conference (p. 4044 (2018)
12. J. Schaefer et al., AIAA Journal **55(1)**, 195-213 (2017)
13. M. Madaliev et al., BIO Web of Conferences **84**, 02032 (2024)
14. Z. M. Malikov, M. E. Madaliev, Vestnik Tomskogo Gosudarstvennogo Universiteta. Matematika i Mekhanika 71, 121-138 (2021)
15. M. Madaliev et al., E3S Web of Conferences **365**, 01011 (2023)
16. Z. M. Malikov et al., Numerical study of an axisymmetric jet based on a new two-fluid turbulence model. AIP Conference Proceedings **2637(1)** (2022)
17. I. Khujaev et al., IOP Conference Series: Materials Science and Engineering **896(1)**, 012046 (2020)
18. I. Khujaev et al., *Research of the elementary section of a gas pipeline under gas outflow from its end to the environment*, in Proceedings of the 2021 International Conference on Information Science and Communications Technologies (ICISCT), pp. 1-4 (2021)
19. Z. M. Malikov, A. A. Mirzoev, M. Madaliev, Journal of Computational Applied Mechanics **53(2)**, 282-296 (2022)
20. M. Madaliev et al., E3S Web of Conferences **508**, 06007 (2024)
21. M. Madaliev et al., E3S Web of Conferences **508**, 06005 (2024)
22. M. Madaliev et al., E3S Web of Conferences **508**, 06003 (2024)
23. E. Son, M. Murodil, Numerical calculation of an air centrifugal separator based on the SARC turbulence model. Journal of Applied and Computational Mechanics (2020)
24. F. R. Menter, Zonal two-equation $k-\omega$ turbulence models for aerodynamic flows. AIAAPaper 1993-2906 (1993)
25. F. R. Menter et al., Ten Years of Industrial Experience with the SST Turbulence Model. Turbulence, Heat and Mass Transfer 4, ed: K. Hanjalic, Y. Nagano, and M. Tummers (Begell House, Inc., 2003)
26. P. Khujaev et al., E3S Web of Conferences **538**, 03019 (2024)
27. P. Khujaev et al., BIO Web of Conferences **84**, 05039 (2024)
28. P. Khujaev et al., E3S Web of Conferences **452**, 04008 (2023)

29. M. Alnaes et al., *Archive of Numerical Software* **3(100)**, 9–23 (2015) DOI: <https://doi.org/10.11588/ans.2015.100.20553>
30. S. Balay et al., *Modern Software Tools for Scientific Computing*, eds. E. Arge, A. M. Bruaset, H. P. Langtangen.– Birkh user Press, pp. 163–202 (1997) DOI: https://doi.org/10.1007/978-1-4612-1986-6_8
31. S. K. Mkhonta et al., *Physical Review Letters* **111(3)**, 035501 (2013) DOI: <https://doi.org/10.1103/PhysRevLett.111.035501>
32. P. K. Galenko et al., *Physical Review B* **83(6)**, 064113 (2011) DOI: <https://doi.org/10.1103/PhysRevB.83.064113>
33. V. Ankudinov, P. K. Galenko, *Journal of Crystal Growth* **539**, 125608 (2020) DOI: <https://doi.org/10.1016/j.jcrysgro.2020.125608>
34. E. Madaliev, et al., *E3S Web of Conferences* **508**, 06001 (2024)
35. M. A. Akhmadaliev et al., *International Polymer Science and Technology* **23(1)**, 34-35 (1996)
36. E. Madaliev et al., Direct numerical simulation of flow in a flat suddenly expanding channel based on nonstationary Navier-Stokes equations. In *AIP Conference Proceedings* **2612(1)** (2023)
37. B. Mirzaev et al., *E3S Web of Conferences* **452**, 06002 (2023)
38. M. Mirzajanov et al., *E3S Web of Conferences* **452**, 06015 (2023)
39. P. Khujaev et al., *E3S Web of Conferences* **538**, 01004 (2024)
40. P. Khujaev et al., *E3S Web of Conferences* **538**, 01010 (2024)